



**HAL**  
open science

## **Bearing fatigue of composite laminates: Damage monitoring and fatigue life prediction**

Cyril Sola, Bruno Castanié, Laurent Michel, Frederic Lachaud, Arnaud Delabie, Emmanuel Mermoz

► **To cite this version:**

Cyril Sola, Bruno Castanié, Laurent Michel, Frederic Lachaud, Arnaud Delabie, et al.. Bearing fatigue of composite laminates: Damage monitoring and fatigue life prediction. *Composites Part B: Engineering*, 2017, 110, pp.487-496. 10.1016/j.compositesb.2016.11.031 . hal-02160873

**HAL Id: hal-02160873**

**<https://hal.science/hal-02160873>**

Submitted on 20 Jun 2019

**HAL** is a multi-disciplinary open access archive for the deposit and dissemination of scientific research documents, whether they are published or not. The documents may come from teaching and research institutions in France or abroad, or from public or private research centers.

L'archive ouverte pluridisciplinaire **HAL**, est destinée au dépôt et à la diffusion de documents scientifiques de niveau recherche, publiés ou non, émanant des établissements d'enseignement et de recherche français ou étrangers, des laboratoires publics ou privés.



## Open Archive Toulouse Archive Ouverte (OATAO)

OATAO is an open access repository that collects the work of some Toulouse researchers and makes it freely available over the web where possible.

This is an author's version published in: <https://oatao.univ-toulouse.fr/24020>

**Official URL :** <https://doi.org/10.1016/j.compositesb.2016.11.031>

### To cite this version :

Sola, Cyril and Castanié, Bruno and Michel, Laurent and Lachaud, Frédéric and Delabie, Arnaud and Mermoz, Emmanuel Bearing fatigue of composite laminates: Damage monitoring and fatigue life prediction. (2017) Composites Part B: Engineering, 110. 487-496. ISSN 1359-8368

Any correspondence concerning this service should be sent to the repository administrator:

[tech-oatao@listes-diff.inp-toulouse.fr](mailto:tech-oatao@listes-diff.inp-toulouse.fr)

# Bearing fatigue of composite laminates: Damage monitoring and fatigue life prediction

Cyril Sola <sup>a, b, \*</sup>, Bruno Castanié <sup>b</sup>, Laurent Michel <sup>b</sup>, Frédéric Lachaud <sup>b</sup>, Arnaud Delabie <sup>a</sup>, Emmanuel Mermoz <sup>a</sup>

<sup>a</sup> Drive Systems Department, Airbus Helicopters, Aéroport Marseille-Provence, 13725 Marignane Cedex, France

<sup>b</sup> Groupe Matériaux et Structures Composites (MSC) Université de Toulouse, UMR CNRS 5312, INSA/UPS/ISAE/Mines Albi, Institut Clément Ader 3 Rue Caroline Aigle, 31400 Toulouse, France

---

## A B S T R A C T

In hybrid composite/metallic structures, loads can be transmitted from one part to the other through localized contact pressures, i.e., bearing. Such structures may be rotating structures, which can accumulate as many as  $10^9$  load cycles during their service life. Designing safe hybrid rotating structures thus requires a sound understanding of how composite joints degrade under bearing fatigue. Pin bearing fatigue tests were run under load control. Damage mechanisms were investigated using computed tomography, and the pin displacement was closely monitored thanks to a green LED micrometer. Building upon the gathered experimental evidences, several damage indicators were then analysed. In particular, hysteresis losses were found to give interesting insights into the fatigue phenomenon, suggesting the existence of a fatigue limit in the very high cycle fatigue (VHCF) regime.

---

### Keywords:

Carbon fibre  
Fabrics/textile  
Fatigue  
Mechanical testing  
Computed tomography

The bearing behaviour of composite joints has been the object of a large number of studies over more than four decades. However, most of these have focused on the strength of bolted assemblies [1–7] and few have dealt with the intrinsic bearing behaviour [8–10]. More recently, some papers investigated the influence of manufacturing flaws on the bearing behaviour, but, again, the scope was mainly limited to bolted joints [11–13]. As new technological opportunities arise [14,15], it is necessary to enhance our knowledge on the consequences of a bearing loading mode, especially for rotating structures subjected to a large number of fatigue cycles, potentially greater than  $10^9$ .

Several studies have shown that the accumulation of permanent hole elongation is the consequence of bearing fatigue damage, and that this elongation can be used as a damage metric [16–19]. Although it has no real influence on the residual strength [18], an excessively large hole elongation can ultimately promote, in pinned or bolted joints, a transition from bearing to more catastrophic failure modes such as shear out or cleavage: it should thus be avoided. Several empirical failure criteria based on hole elongation

have been proposed. However, depending on the layup or other factors, the critical permanent hole elongation ranges from 4% of the hole diameter [12,20] to as much as 10% [21]. Furthermore, it is not known whether hole elongation build up can be stopped or not, i.e., whether there is a practical fatigue limit (or endurance limit) or not. In most bearing fatigue tests reported in the literature, run out was considered when the fatigue life exceeded  $10^6$  cycles. In this fatigue domain, the S N curve had no asymptote [21–23]. Another question that arises is whether the residual stiffness evolves significantly in fatigue, which could prove critical for stiffness driven applications. In particular, Smith and Pascoe [17] suggested that, for crossply laminates, very long lives would imply a very low residual stiffness.

The first objective of this study was to understand the different fatigue damage mechanisms involved when CFRP laminates are subjected to bearing loads. A simple test set up and coupon were selected with the aim of focusing on this peculiar loading mode. The main macroscopic consequence of damage was an incremental collapse behaviour, or ratcheting, which explains why permanent hole elongation can be used to monitor the fatigue damage evolution in pinned or bolted joints, just as under monotonic loads. The second part of the paper investigates the capabilities of this damage metric regarding lifetime prediction. It also considers other damage

---

\* Corresponding author. Drive Systems Department, Airbus Helicopters, Aéroport Marseille-Provence, 13725 Marignane Cedex, France.

E-mail address: [cyril.sola@airbus.com](mailto:cyril.sola@airbus.com) (C. Sola).

indicators, such as residual stiffness and hysteresis losses. In the last part of the article, the analysis of the experimental trends and damage metrics are used to assess the possible existence of a fatigue limit.

## 1. Materials and methods

Half hole bearing tests were chosen. This set up enabled friction to be minimized so as to prevent heat build up. This test is similar to the pinned bearing test which essentially differs from the bolt bearing one in that there is no out of plane restraint. The pin, or indenter, was the reamer that had been used to ream the holes in the composite coupons. Half hole bearing tests were successfully used in a previous study focusing on the bearing behaviour under monotonic loads [24] (see Fig. 1 and Fig. 2).

Fatigue tests were performed at 10 Hz, a frequency sufficiently low to avoid excessive elevation of the temperature. Temperature measurements obtained with an infrared camera showed that the increase in the surface temperature of the coupons was lower than 10 °C, even after thousands of cycles.

The coupons were made of carbon fibre prepreg with a UD fabric or 4 harness satin weave fabric. The chosen layup was quasi isotropic and symmetric, with  $[90,45,0, 45]_{ns}$  ply sequences. The number of sequences  $n$  was adapted so that the UD and woven laminates would have equivalent thicknesses, close to 4 mm.

Tests were load controlled as, with displacement control, obtaining a clear failure<sup>1</sup> would have been close to impossible because of the expected build up of permanent hole elongation, that could ultimately have led the coupon to not being loaded any longer. Load ratios ( $R = F_{min}/F_{max}$ ) of 10 and 3 were selected in order to assess the mean load influence. This choice implied that the coupons were never completely unloaded; a small preload was always present. Therefore, debris that were generated as a result of wear were not evacuated and remained trapped between the pin and the hole. This was initially a concern, as Grant and al [18], had shown that the presence of debris could affect fatigue life. However, the amount of debris was later found to be negligible.

For a given material, three coupons were tested to failure for each chosen load amplitude. A minimum of three load amplitudes was selected to generate each of the four S N curves corresponding to the two materials and the two load ratios. The maximum absolute load in a cycle  $|F_{min}|$  was in the range  $[0.65 \cdot |F_{ultimate}|, 0.93 \cdot |F_{ultimate}|]$  for the woven fabric laminates and  $[0.7 \cdot |F_{ultimate}|, 0.94 \cdot |F_{ultimate}|]$  for the UD fabric laminates. The initial test matrix is shown in Table 1. A few extra data points were added to this matrix later.

The pin displacement was measured, without contact, with a Keyence LS7030 green LED micrometer (see Fig. 3). Displacement and force were both sampled at 200 Hz, so 20 lines of data were available for each fatigue cycle.

Under load control, fatigue failure was sudden. Hence, there was no need to define a fatigue failure criterion as a certain amount of permanent hole elongation or stiffness decrease.

## 2. Damage mechanisms

### 2.1. Incremental collapse: a macroscopic consequence of damage

Upon fatigue loading, a permanent hole elongation gradually accumulates. In the current study, this damage metric was estimated as shown on Fig. 4. It can be noted that this damage metric is closely related to the fatigue modulus of Hwang and Han [25].

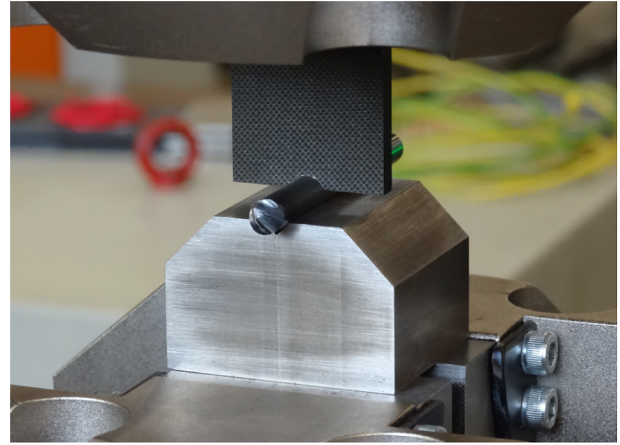


Fig. 1. Half-hole bearing test set-up.

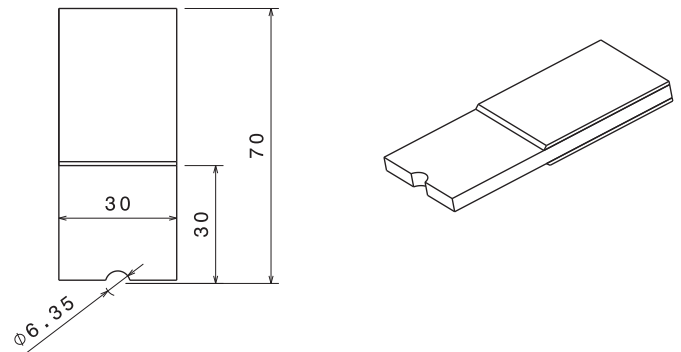


Fig. 2. Coupon geometry. Both UD-fabric and woven fabric coupons were about 4 mm thick.

The increase in permanent hole elongation followed three stages. The first stage was probably a run in stage; the permanent hole elongation increased quickly. The second stage was characterized by a linear increase of the permanent hole elongation. Finally, the hole elongation increased exponentially as final failure occurred. Interestingly, the permanent hole elongation evolution curve followed the same trend as the well known damage evolution curve of a unidirectional laminate under tensile loading, where the transition from stage 1 to stage 2 coincides with the so called “Critical Damage State” (CDS) [26]. When plotted as a function of the normalized number of cycles  $N/N_f$ , where  $N_f$  is the number of cycles to failure, the permanent hole elongation appeared to have a critical threshold value around  $50 \mu\text{m} - 60 \mu\text{m}$ , i.e., slightly less than 1% of the hole diameter. Once this value was exceeded, failure occurred in a matter of a few cycles, typically less than 10% of the total fatigue life, though some coupons had a much larger residual life after reaching the threshold (Fig. 5).

It should be noted that this critical value is very close to that reported by Seike et al. [22], despite the different test set up and materials (but the similar pin diameter and quasi isotropic layups). The permanent hole elongation curve has the same shape irrespective of the load ratio. When expressed as a fraction of the total fatigue life, the three stages have constant durations. The first stage typically represents less than 10% of the fatigue life, 80% is accounted for by the second stage, and the last 10% corresponds to the final failure stage.

<sup>1</sup> Characterized by a sharp load drop.

**Table 1**  
Fatigue test matrix.

Test type	Coupon type	R-ratio	$ F_{min} $	No. of specimens
Fatigue	UD-fabric	10	$ F_{min}  \approx 0.94 \cdot  F_{ultimate} $	3
Fatigue	UD-fabric	10	$ F_{min}  \approx 0.85 \cdot  F_{ultimate} $	4
Fatigue	UD-fabric	10	$ F_{min}  \approx 0.78 \cdot  F_{ultimate} $	3
Fatigue	UD-fabric	10	$ F_{min}  \approx 0.71 \cdot  F_{ultimate} $	3
Fatigue	UD-fabric	3	$ F_{min}  \approx 0.86 \cdot  F_{ultimate} $	3
Fatigue	UD-fabric	3	$ F_{min}  \approx 0.81 \cdot  F_{ultimate} $	3
Fatigue	UD-fabric	3	$ F_{min}  \approx 0.78 \cdot  F_{ultimate} $	3
Fatigue	Woven fabric	10	$ F_{min}  \approx 0.93 \cdot  F_{ultimate} $	3
Fatigue	Woven fabric	10	$ F_{min}  \approx 0.78 \cdot  F_{ultimate} $	3
Fatigue	Woven fabric	10	$ F_{min}  \approx 0.73 \cdot  F_{ultimate} $	3
Fatigue	Woven fabric	10	$ F_{min}  \approx 0.65 \cdot  F_{ultimate} $	3
Fatigue	Woven fabric	3	$ F_{min}  \approx 0.90 \cdot  F_{ultimate} $	3
Fatigue	Woven fabric	3	$ F_{min}  \approx 0.85 \cdot  F_{ultimate} $	3
Fatigue	Woven fabric	3	$ F_{min}  \approx 0.80 \cdot  F_{ultimate} $	3
Fatigue	Woven fabric	3	$ F_{min}  \approx 0.77 \cdot  F_{ultimate} $	3
Fatigue, stopped at $10^6$ cycles	UD-fabric	10	$ F_{min}  \approx 0.54 \cdot  F_{ultimate} $	1
Fatigue, stopped at $10^6$ cycles	Woven fabric	10	$ F_{min}  \approx 0.53 \cdot  F_{ultimate} $	1
Fatigue, stopped at 1st characteristic point <sup>a</sup>	UD-fabric	10	$ F_{min}  \approx 0.81 \cdot  F_{ultimate} $	1
Fatigue, stopped at 2nd characteristic point	UD-fabric	10	$ F_{min}  \approx 0.81 \cdot  F_{ultimate} $	1
Fatigue, stopped at 3rd characteristic point	UD-fabric	10	$ F_{min}  \approx 0.81 \cdot  F_{ultimate} $	1
Fatigue, stopped at 1st characteristic point	Woven fabric	10	$ F_{min}  \approx 0.81 \cdot  F_{ultimate} $	1
Fatigue, stopped at 2nd characteristic point	Woven fabric	10	$ F_{min}  \approx 0.81 \cdot  F_{ultimate} $	1
Fatigue, stopped at 3rd characteristic point	Woven fabric	10	$ F_{min}  \approx 0.81 \cdot  F_{ultimate} $	1

<sup>a</sup> See section 2.2 for the definition of characteristic points.

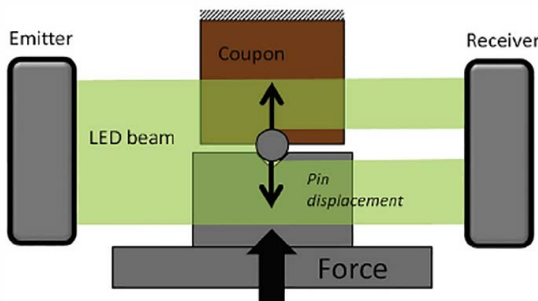


Fig. 3. The pin displacement was measured with a green LED micrometer.

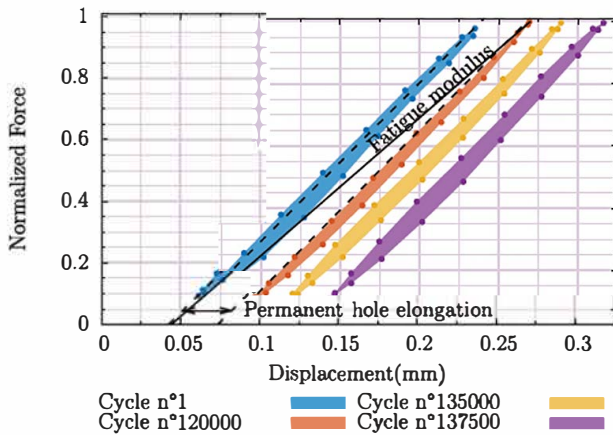


Fig. 4. The permanent hole elongation was estimated as shown on the graph (UD-fabric laminate in this case). It is closely related to the fatigue modulus, sometimes used as a damage metric [25,32].

## 2.2. Ply level damage: the role of kinking

Each coupon has its own permanent hole elongation curve, but for any such curve, three characteristic points can be defined, as shown on Fig. 6. For woven and UD fabric laminates, three tests

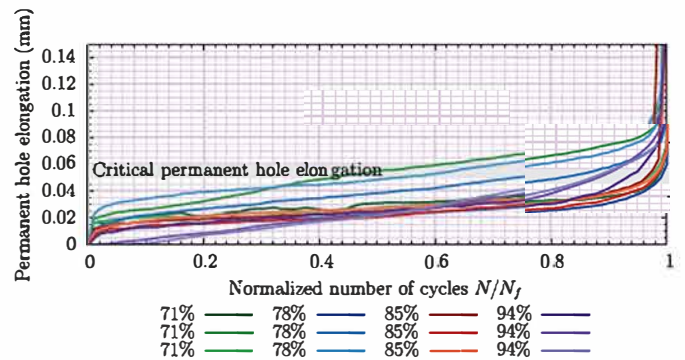


Fig. 5. Increase in the permanent hole elongation. The percentages correspond to the ratio  $|F_{min}|/|F_{ultimate}|$ , where  $|F_{ultimate}|$  was estimated using 12 static tests.

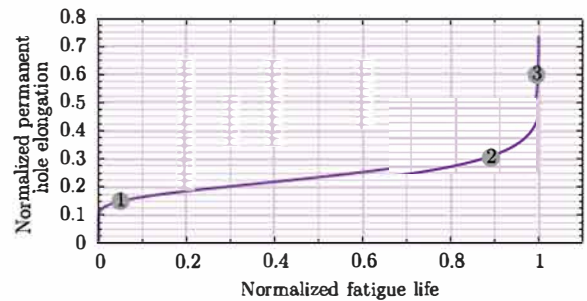


Fig. 6. Three characteristic points were chosen on the typical permanent hole elongation curve and some fatigue tests were stopped at each of these points.

were definitively stopped at each of these points, so as to obtain coupons with different fatigue damage levels. The coupons were CT scanned in a GE Phoenix VTome XM microtomograph.

It was deemed that the nature of fatigue damage was independent of the load level. In the stopped tests,  $|F_{min}|$  was rather high, representing 81% of the mean static failure load,<sup>2</sup> but the

<sup>2</sup> Evaluated with 12 static tests.

short test duration enabled the evolution of the permanent hole elongation to be monitored closely and tests to be stopped at the most appropriate moment. It should be noted that, at this load level, damage could initiate at the first fatigue cycle, as static damage typically starts at about 70% of the static failure load [24]. Just after the run in phase, kink bands were found in all the 0° plies and close to the hole surface. Locally bent packs of fibres and inter fibre cracks probably paved the way for kink band initiation upon further loading (Fig. 7). At this stage, delaminated areas were almost non-existent. Therefore, most of the initial permanent hole elongation could be attributed to these local damage mechanisms in the load bearing plies, at, or in the close vicinity of, the hole surface.

At the second characteristic point, coupons were highly

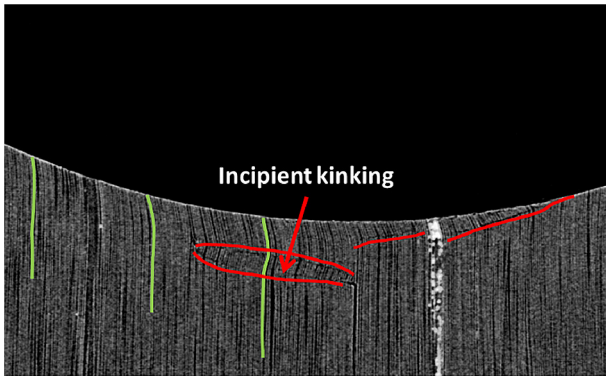


**Fig. 7.** Local damage mechanisms that develop during stage 1 explain the initial increase in permanent hole elongation. At this stage, kink bands are rarely fully developed; therefore, they can be referred to as “incipient” kink bands.

damaged. Kink bands were found in both 0° and ±45° plies. Shear driven compressive failure was also noticed (Fig. 8), especially in ±45° plies. Delaminations were essentially located in the outer ply sequences. It appeared that delaminations initiated mainly as a result of wedge mechanisms triggered by kinking. The incremental collapse behaviour was most probably connected with the progressive development of kink bands throughout the whole course of the damage process. Kink bands obviously engendered residual strains, particularly when they collapsed upon repeated loading, which seems to have happened for many of them, especially in the last stages of the fatigue life (characteristic point n°3, Fig. 9). The complete fatigue failure scenario in the so called *bearing plane*, i.e., the plane dividing the coupon width into two equal parts, is shown in Fig. 10. No clear difference was noted between woven and UD fabric laminates: kink bands and delaminations explained the final failure in both cases.

Finally, the second stage of damage evolution, delimited by the first and second characteristic points, was characterized by the stable development of kink bands, which tended to more and more offset from the hole surface. As long as these kink bands did not trigger out of plane cracks, the increase in permanent hole elongation was small because the greater presence of kink bands at a certain distance from the hole probably only marginally affected the local behaviour at the pin/hole interface, where damage initiated before the first characteristic point and clearly affected the contact surface.

To investigate the nature of fatigue damage when fatigue loads did not exceed the static initiation load of kink bands, fatigue tests were performed at low load levels (with  $|F_{min}| = 0.54 \cdot |F_{ultimate}|$ ) and stopped after  $10^6$  cycles. Although matrix cracks were present, especially in the outer ply sequences, no proper kink bands were noticed (although some packs of fibres had apparently bent under load close to the hole surface). Permanent hole elongation was

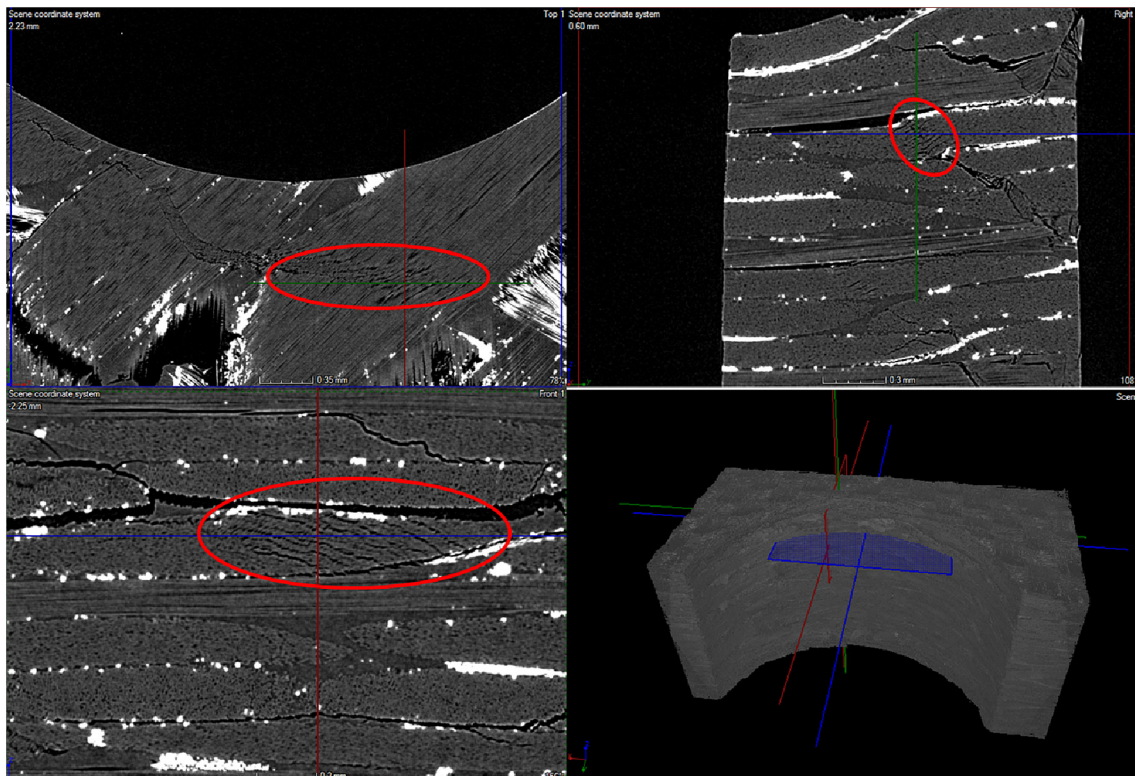


**Fig. 8.** Shear driven compressive fibre failures were sometimes observed.

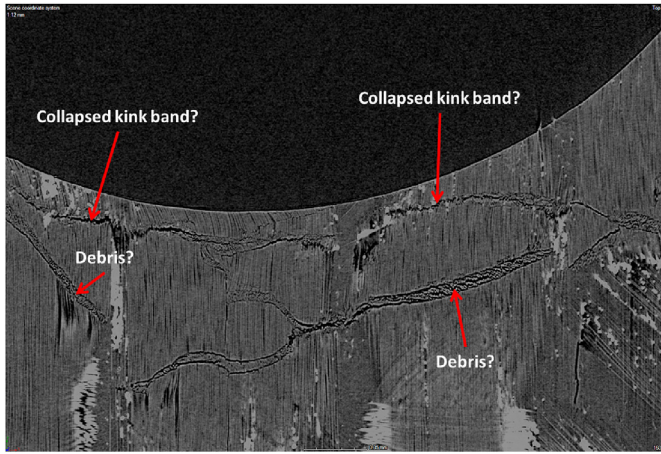


**Fig. 9.** At stage 3, kink bands appear to ultimately collapse as fibre debris are generated in the bands due to repeated loading.

found to be insignificant (lower than  $10\ \mu\text{m}$ ). However, it increased slightly but steadily at the very beginning of the fatigue test (before  $10^5$  cycles), remaining almost constant thereafter, which suggested a long residual life.

Therefore, it is very clear that permanent hole elongation can be used as a damage metric, but a question arises: is it the only possibility, and how would it compare to other damage metrics, should

they exist? Residual stiffness and hysteresis losses, which are necessarily related to the amount of fatigue damage, come to mind. Since fatigue damage develops so early in the fatigue life, clear trends should emerge. The purpose of the following section is to investigate these points.

### 3. Evaluation of different damage parameters

#### 3.1. Stiffness as a damage parameter

Residual stiffness has long been used to monitor damage evolution in composite laminates. When it comes to bearing, the study by Smith and Pascoe [17] promoted this damage metric as a valuable alternative to permanent hole elongation measurements, which they deemed difficult to carry out. However, their study dealt with cross ply laminates, which do not behave like quasi isotropic laminates. In addition, the coupons they used were not half hole specimens, and this is also a significant difference with respect to the current study.

For the quasi isotropic laminates of our study, the residual stiffness was not a very interesting damage metric as it did not change significantly with increasing cycle count. It increased at the very beginning of the fatigue life, and then decreased progressively for most of the lifetime up to the final failure (Fig. 11). In most cases, after reaching its peak value, stiffness did not decrease by more than 4%, and in some cases, the residual stiffness could even remain almost constant for the whole fatigue life. The initial increase in the

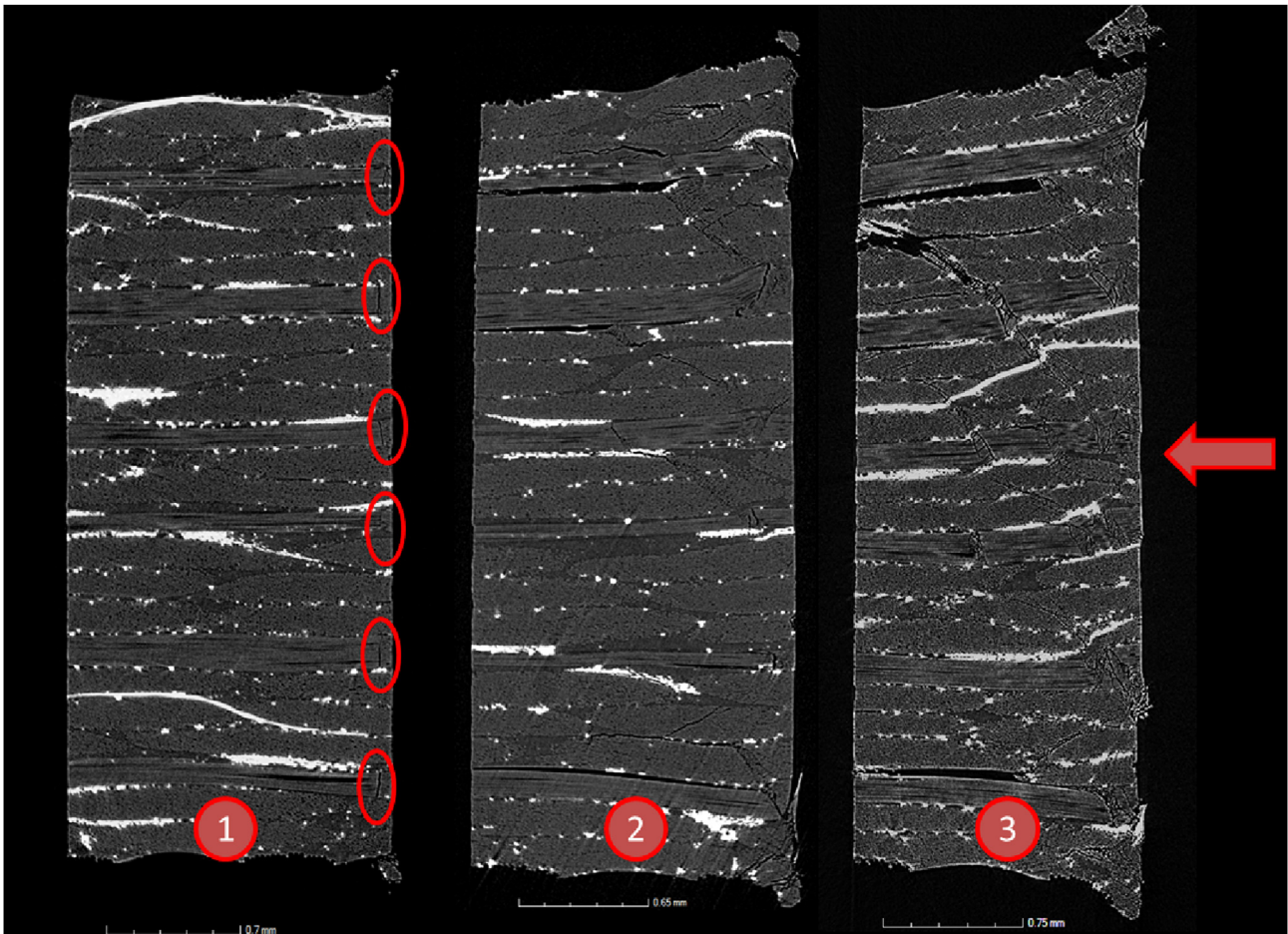


**Fig. 10.** Fatigue damage evolution for the three characteristic points. UD-fabric laminate.

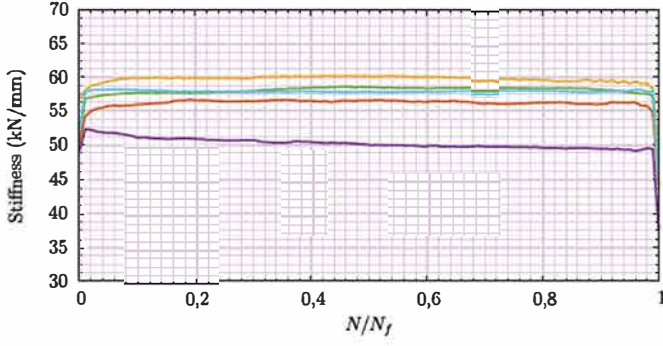


Fig. 11. Stiffness variations for six UD-fabric coupons with  $R = 10$ . Stiffness was calculated for each individual cycle, which explains the slight oscillations.

residual stiffness was attributed to a run in phenomenon, during which the composite contact surface was assumed to adapt itself to the pin surface by wearing slightly, ultimately resulting in an increased contact surface. High initial stiffness was not positively correlated with longer fatigue lives. Should such an effect exist, it would be difficult to demonstrate as it could be masked by slight variations in the gauge length of the coupon, which was not carefully controlled, as it was considered a non critical parameter.

### 3.2. Hole elongation as a damage parameter

Being characterized by a three stage evolution, the permanent hole elongation evolution can be described by the Wu and Yao model [26], which was originally designed to describe damage evolution in a tension loaded unidirectional laminate. It can be assumed that the permanent hole elongation  $v$  is directly proportional to damage  $D$ , so equation (1) holds.

$$v = k \cdot D = k \cdot \left( 1 - \left( 1 - \left( \frac{N}{N_f} \right)^a \right)^b \right) \quad (1)$$

It should be noted that the parameter  $k$  can be chosen arbitrarily, as it only acts as a scaling parameter, transforming the adimensional damage variable into a length. The main interest of the previous equation is that it can be used to predict the fatigue life if  $v$  after  $N$  fatigue cycles is known. It could also be used to generate master curves that would prove very useful if a FE damage model were to be developed, by making it possible to check the credibility of the simulated permanent hole elongation curve, irrespective of the number of cycles to failure.

$$N_f = N \left( 1 - \left( 1 - \frac{v}{k} \right)^{\frac{1}{b}} \right)^{-\frac{1}{a}} \quad (2)$$

Of course, to do this, the parameters  $a$  and  $b$  should preferably only depend on the test configuration (load amplitude,  $R$  ratio, etc.), through a mathematical expression that needs to be defined. In this regard, it can be considered that the parameter  $a$  is related to the load through a power law. This parameter mainly controls the shape of the curve in the initial run in stage. A lower  $a$  means a higher initial increase in the permanent hole elongation. It has been noticed that  $a$  tends to be smaller as fatigue life becomes longer. Therefore, long fatigue lives seem to be positively correlated with a high initial increase of the permanent hole elongation.

$$a = A \left( \frac{|F_{min}|}{|F_{ultimate}|} \right)^B \quad (3)$$

The parameter  $b$  does not seem to be related to any test

parameter. However, as  $b$  mainly controls the shape of the evolution curve in the vicinity of  $N_f$ , it can be expressed as a function of a critical permanent hole elongation value  $V$ , reached at some specific  $N/N_f$  ratio close to 0.9. However, since this critical value is not reached at exactly the same  $N/N_f$  ratio for all fatigue tests, variations around this ratio should be considered. Therefore, only an envelope of the true fatigue behaviour can be obtained. As a result, the predictive abilities of the model are considerably reduced. Even if the parameters  $a$  and  $b$  are made dependent from the number of cycles to failure  $N_f$ , as originally suggested by Wu and Yao, it is not possible to find a law that enables accurate values of  $a$  and  $b$  to be obtained for a given test configuration, without having to perform curve fitting.

$$b = \frac{\ln\left(1 - \frac{V}{k}\right)}{\ln\left(1 - \left(\frac{N}{N_f}\right)^a\right)} \quad (4)$$

A more interesting approach is to evaluate the derivative of equation (1) for  $N/N_f = 0.5$ , which corresponds to the permanent hole elongation accumulation rate at mid life, i.e., in the second stage of damage development. Since the permanent hole elongation increases almost linearly for the whole of stage 2, it can be considered that, for this stage,  $dv/dN$  is constant. Therefore, if the permanent hole elongation rate is estimated experimentally at the beginning of stage 2, it can be directly identified to  $dv/dN$  evaluated for  $N/N_f = 0.5$ .

It was found that  $dv/dN$  evaluated for  $N/N_f = 0.5$  could be related to  $N_f$  through an inverse power law (Fig. 12).

This result means that the fatigue life can be easily predicted, as long as the permanent hole elongation accumulation rate is known once stage 2 is reached. A proper fatigue life estimation is, however, difficult when fatigue lives are greater than  $10^6$  cycles. In this particular case, the permanent hole elongation accumulation rate is extremely low in stage 2, which makes its experimental estimation tricky. Moreover, unless a very large number of cycles have been performed, it is not trivial to determine whether stage 2 has been reached or not. Should this not be the case, the life prediction would be overly conservative. Thus, this model is best suited to the analysis of fatigue data with  $N_f$  ranging from  $10^2$  to  $10^6$  cycles. The capabilities of the method are shown on Fig. 13. The predictions were made using fatigue data limited to  $N \leq 0.33 \cdot N_f$ , i.e., limited to stage 1 and the beginning of stage 2. Finally, it has to be acknowledged

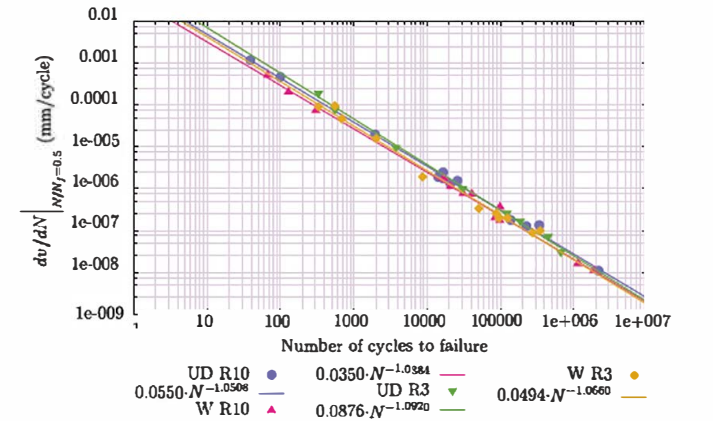


Fig. 12. The permanent hole elongation accumulation rate, evaluated for  $N/N_f = 0.5$ , can be obtained through an inverse power law, where the independent variable is the number of cycles to failure. Therefore, the fatigue life of a given coupon can be predicted as long as the stage 2 permanent hole elongation accumulation rate is known.

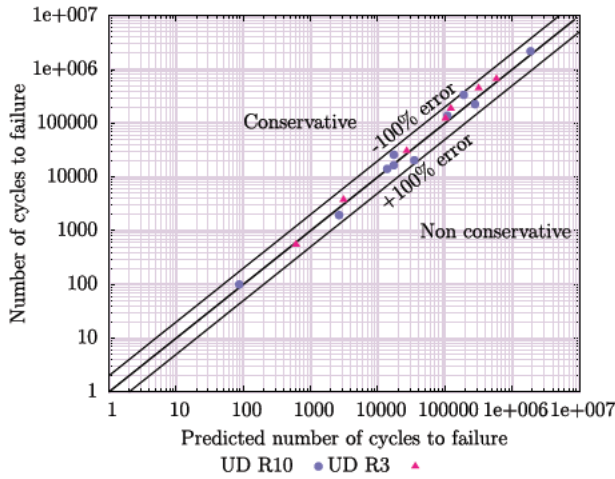


Fig. 13. A fair correlation between the predicted and experimental fatigue lives for UD-fabric laminates was obtained using a method based on the permanent hole elongation accumulation rate.

that the prediction of the fatigue behaviour in stage 1 is extremely difficult, because it most probably relates to very local laminate properties, which are closely connected to the hole drilling process and how the tows are arranged, among other things.

### 3.3. Hysteresis energy as a damage parameter

The area enclosed in the hysteresis loops corresponds to hysteresis energy, i.e., dissipated energy. Energy dissipation in composites can mainly be attributed to viscosity and to damage [27]. In the specific case of bearing, friction between the pin and the hole adds to these dissipative mechanisms. Therefore, hysteresis losses could be used to monitor damage evolution. This energy was calculated for each cycle by a simple trapezoidal integration of the load displacement loop.

As is the case with stiffness and permanent hole elongation, the evolution of the hysteresis energy in a load controlled fatigue test is characterized by three stages. In the first one, hysteresis energy decreases steadily, then it stabilizes for most of the fatigue life, before increasing slightly just before final failure. The remarkable stability of the hysteresis energy implies that the cumulative hysteresis energy is almost linearly related to the stabilized hysteresis energy, and that the mean hysteresis energy can be considered equal to the stabilized hysteresis energy. This stability also suggests that most of the energy is simply dissipated as heat through viscous mechanisms, in a non evolving fashion, unlike the situation with damage. This would be consistent with the findings of Erber and Guralnick [28], who showed that, for metallic materials, the energy dissipated due to damage only represented a very small proportion of the total hysteresis losses despite the absence of significant viscoelasticity. Last but not least, the stability of the hysteresis losses *apparently* means that, like residual stiffness, hysteresis energy cannot serve as an effective damage parameter.

However, hysteresis energy does relate to fatigue life. It was found that, in a log log diagram, the cumulative hysteresis energy to failure (which from now on will also be called the *critical cumulative hysteresis energy*) was linearly related to the number of cycles to failure (Fig. 14), meaning that the latter is the independent variable of a power law. This relationship does not seem to be very sensitive to the fabric type. It is, however, sensitive to the R ratio and to the test frequency.

It is possible to estimate the fatigue life of a coupon by resorting to the property of linear accumulation of the hysteresis energy.

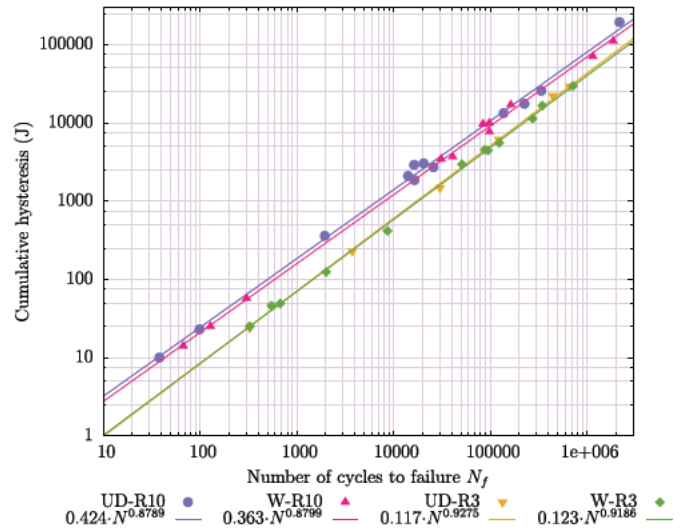


Fig. 14. The cumulative hysteresis to failure is linearly related to the number of cycles to failure in a log-log diagram. In the plot key, UD stands for UD-fabric and W stands for woven fabric. Note that when the R-ratio is identical, UD and W laminates behave similarly.

Fatigue failure is assumed to occur once the cumulative hysteresis energy exceeds the critical cumulative hysteresis energy  $H_{critical}$  for given R ratio and frequency, i.e.:

$$H_{critical} = H_m \cdot N_f \tag{5}$$

where  $H_m$  is the mean hysteresis energy. This life prediction method is illustrated in Fig. 15.

The analysis of the evolution of the mean hysteresis energy with respect to the alternating load provides other interesting insights into the fatigue behaviour. Using the data extracted from tests that were run up to final failure, this analysis suggested that hysteresis might vanish at low load amplitudes, a phenomenon that would strongly imply the existence of fatigue limit. To further investigate this, new data points were necessary but, because of the low load levels that were required for this purpose, running the

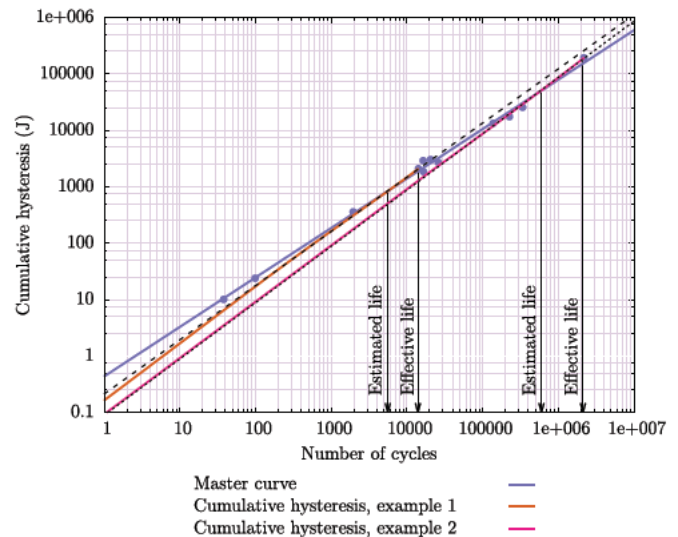


Fig. 15. Fatigue life estimation based on equation (5). Examples 1 and 2 refer to the cumulative hysteresis curve of individual coupons. The intersection of these curves with the master curve yields the estimated fatigue life for both examples.

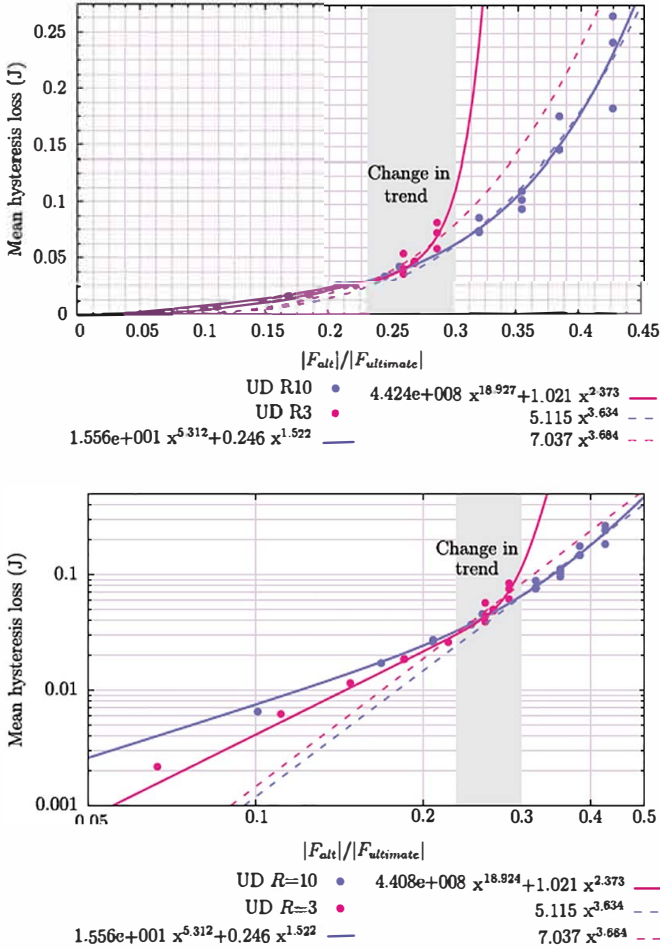


Fig. 16. There is a change in trend in the evolution of the mean hysteresis loss as a function of the alternate load. For low load levels, this evolution cannot be described by a single power law (dotted lines). To bring this out more clearly, the data were plotted in a log-log diagram (second graph). Referring to Fig. 19, the change in trend region can clearly be associated with the frontier between high cycle and very high cycle fatigue ( $N_f \geq 10^8$ ).

corresponding fatigue tests up to final failure was out of the question. Consequently, the mean hysteresis energy for low alternating load was estimated on the basis of fatigue tests that were stopped at  $10^5$  cycles.

This investigation showed that hysteresis never completely vanished. However, two different trends emerged, so the experimental data points could be fitted by a function that was a sum of two power laws (Fig. 16). This probably means there was a shift in the way energy was dissipated. Dissipation might have occurred essentially through viscous mechanisms at low load levels, and damage would then play a more and more important role as the alternating load increased. Referring to an S N curve (see Fig. 17 for example), the change in trend can clearly be associated with the frontier between the HCF and the VHCF ( $N_f \geq 10^8$ ) fatigue regimes. The existence of a fatigue limit still remains to be debated.

#### 4. Does a bearing fatigue limit exist?

Although no true fatigue limit really exists for metallic materials [29], it is well known that, for most of them, the S N curve becomes asymptotic in the VHCF fatigue regime. Assessing the existence of such asymptotic behaviour in composite materials is extremely difficult, as the self heating phenomenon usually imposes test

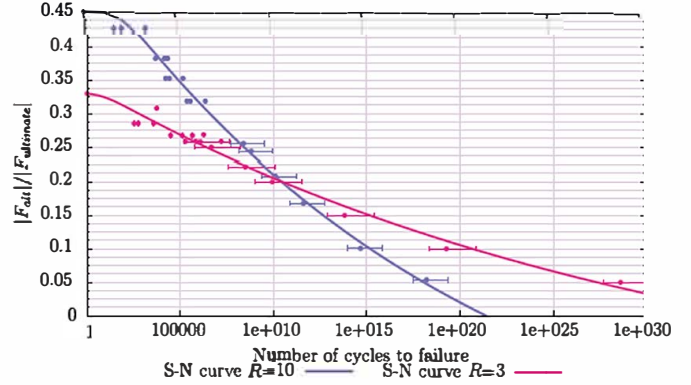


Fig. 17. Based on the knowledge of the mean hysteresis loss for low load levels and using the equations linking the critical cumulative hysteresis to the number of cycles to failure, it is possible to estimate the number of cycles to failure of coupons expected to fail in the VHCF regime (points with error bars). Points without error bars correspond to coupons cyclically loaded until fatigue failure. The fitted S-N curves do not take the error bars into account, as errors are asymmetric.

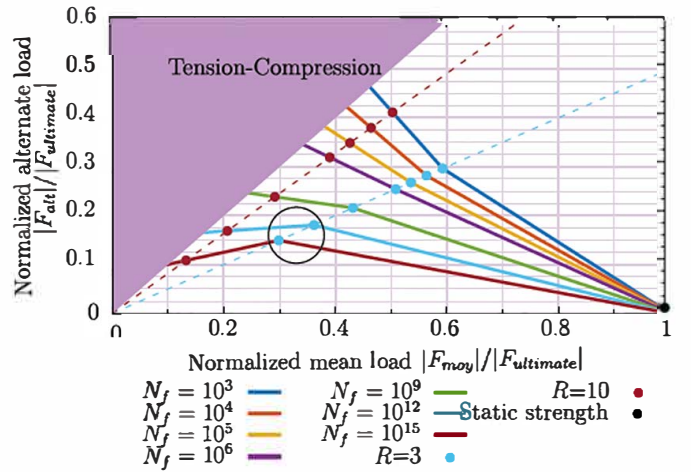


Fig. 18. Should the S-N curves cross, a knee point would appear in the CLD diagram (circled area), translating the fact that, despite lower mean and alternating loads, the fatigue life for  $R = 10$  could end up being the same as for  $R = 3$ .

frequencies that would make VHCF test durations prohibitive. At 10 Hz, almost 116 days would be required to reach  $10^8$  cycles. Therefore, considering the lack of experimental evidence, the existence of a fatigue limit for composite materials has long been debated [30]. Some arguments suggesting the possible existence of a bearing fatigue limit are put forward below.

The first and main argument is *reductio ad absurdum*, which is based on the following observation:

The S N curves obtained for two R ratios should cross for a large number of cycles, with the S N curve for  $R = 3$  ultimately staying above the S N curve for  $R = 10$  (Fig. 17).

Therefore, for low load levels, the same fatigue life would be expected for  $R = 10$  and  $R = 3$  despite the lower mean load and alternating load for  $R = 10$ . This would translate into an absurd Constant Life Diagram, with a knee point (Fig. 18). To prevent this, the S N curves at  $R = 3$  and  $R = 10$ , plotted as the alternating load  $|F_{alt}|$  versus  $N_f$ , should converge towards the same limit, or, at least, evolve in the same fashion. In the latter case, it would be more logical for the S N curves to become less steep, as there is little chance of the damage kinetics accelerating in the high cycle regime.

The second argument is that, when all fatigue and static failure points are considered, and when woven and UD fabric data points

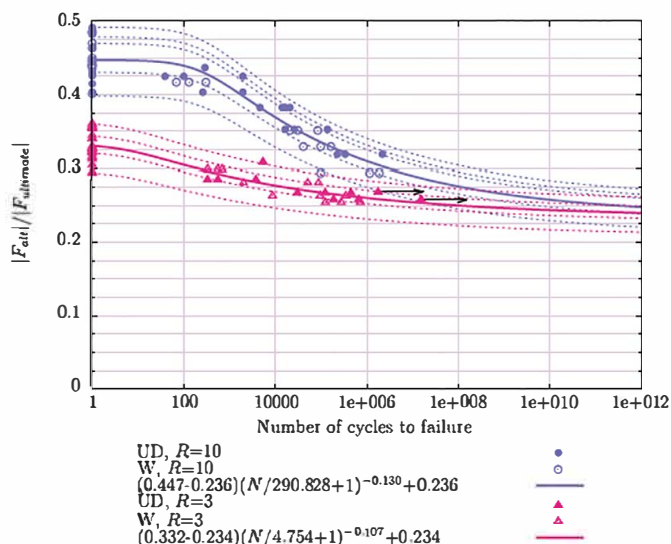


Fig. 19. The S-N curves might have a horizontal asymptote in the VHCF regime. If they were not asymptotic nor superposed, they would cross, resulting in an absurd CLD diagram (Fig. 18). The arrows indicate runout.

are pooled together, so as to increase the number of data points,<sup>3</sup> a Weibull equation fits the experimental data points fairly well (Fig. 19). Although this equation implies a fatigue limit, the true existence of a fatigue limit for  $R = 10$  is difficult to infer from this analysis alone, even though it seems to be rational for  $R = 3$ , especially when the two run out tests are considered. It is interesting to note that the Weibull equation suggests the existence of different coupon families, with coupons having the highest static strength also having the highest fatigue strength (see the dotted lines on Fig. 19). This fact is consistent with the SLERA (Stress Life Equal Rank Assumption) theory [31], which states that static and fatigue strengths are correlated, making it a sensible argument in favour of the Weibull equation.

A third argument is the fact that, under monotonic loading, kinking only starts when the bearing load reaches 70–75% of the failure load. Therefore, when the applied fatigue load  $|F_{min}|$  is close to this threshold,<sup>4</sup> the fatigue life is very long, because kinking has to be triggered and has to affect a certain material volume before fatigue failure can occur. The suspected fatigue limit is such that the corresponding  $|F_{min}|$  load is below the load at which kink bands initiate in static, for both  $R$  ratios. Hence, since fatigue life can be very long when  $|F_{min}|$  is slightly above this threshold ( $N_f > 10^7$  for  $R = 3$ ), it can be expected that, when it is below, no fatigue failure would occur before a much higher number of cycles, supporting the idea that a practical fatigue limit might exist. Although fatigue failure seemingly occurred below the kink band initiation threshold on some occasions, this might not have actually been the case. In fact, in most fatigue tests, the peak load  $|F_{min}|$  exceeded the threshold, even at low load levels, the scatter in static strength being rather large when evaluated on a large number of coupons ( $>10$ ). The possibility should also be considered that, even if the peak fatigue load exceeds the static initiation threshold, the load amplitude might be too small to significantly damage the coupons. This is what appeared to happen with  $R = 3$ , as no fatigue failure was obtained for peak loads falling into the kink bands static

<sup>3</sup> Which is reasonable, as these points fell within similar scatter bands.

<sup>4</sup> In fatigue, this threshold corresponds to  $|F_{alt}|/|F_{ultimate}| \geq 0.31$  ( $R = 10$ ) or 0.23 ( $R = 3$ ), see Fig. 19.

initiation load band.

The last argument refers to the change in trend in the evolution of the mean hysteresis loss as a function of the alternating load, which was observed in Fig. 16.

## 5. Conclusions

The fatigue life of quasi isotropic laminates subjected to bearing loads can be predicted using damage parameters such as the permanent hole elongation accumulation rate or the cumulative hysteresis energy. Using such damage metrics, clear trends can be obtained. The permanent hole elongation is difficult to measure and, as is the case with cumulative hysteresis losses, fatigue data need to be post processed. However, it relates directly to the amount of damage, whereas hysteresis energy encompasses not only damage but also other dissipative phenomena such as visco elasticity. Both damage metrics can be used to predict the fatigue life based on a limited amount of fatigue data, typically accounting for less than 30% of the total fatigue life. To achieve an in service prediction of the residual fatigue life, a monitoring system should be implemented. The measurement of a given damage metric, either directly or indirectly, would then be possible. But such a system is still utopic, especially for rotating structures or components. A more down to earth application of these damage metrics would be to evaluate the capabilities of a damage model. Indeed, those would be useful to assess the consistency of the predicted damage rates or hysteresis losses, which would be key if the model in question were to be used to predict the fatigue life under spectral loadings. Finally, even though the existence of a fatigue limit has not been proven, the different analyses strongly suggest that a *practical* fatigue limit does seem to exist. No fatigue failure would occur for alternating loads lower than about 20% of the static failure load, since, at this load level, the expected fatigue lives are clearly located in cycle ranges that are not susceptible of being reached in any known industrial application. It has been shown that this practical fatigue limit is closely related to the static initiation load of kink bands, in full consistency with the fact that the latter drive the fatigue failure process.

## References

- [1] Thoppul SD, Finegan J, Gibson RF. Mechanics of mechanically fastened joints in polymer matrix composite structures: a review. *Compos Sci Technol* 2009;69(3–4):301–29. <http://dx.doi.org/10.1016/j.compscitech.2008.09.037>.
- [2] McCarthy MA. An experimental study of bolt-hole clearance effects in single-lap, multi-bolt composite joints. *J Compos Mater* 2005;39(9):799–825. <http://dx.doi.org/10.1177/0021998305048157>.
- [3] Warren KC, Lopez-Anido RA, Vel SS, Bayraktar HH. Progressive failure analysis of three-dimensional woven carbon composites in single-bolt, double-shear bearing. *Compos Part B Eng* 2016;84:266–76. <http://dx.doi.org/10.1016/j.compositesb.2015.08.082>.
- [4] Gray P, O'Higgins R, McCarthy C. Effects of laminate thickness, tapering and missing fasteners on the mechanical behaviour of single-lap, multi-bolt, countersunk composite joints. *Compos Struct* 2014;107:219–30. <http://dx.doi.org/10.1016/j.compstruct.2013.07.017>.
- [5] Khashaba U, Sebaey T, Alnefaie K. Failure and reliability analysis of pinned-joints composite laminates: effects of stacking sequences. *Compos Part B Eng* 2013;45(1):1694–703. <http://dx.doi.org/10.1016/j.compositesb.2012.09.066>.
- [6] Aktaş A. Bearing strength of carbon epoxy laminates under static and dynamic loading. *Compos Struct* 2005;67(4):485–9.
- [7] Kelly G, Hallstrom S. Bearing strength of carbon fibre/epoxy laminates: effects of bolt-hole clearance. *Compos Part B Eng* 2004;35(4):331–43. <http://dx.doi.org/10.1016/j.compositesb.2003.11.001>.
- [8] Ascione F, Feo L, Maceri F. An experimental investigation on the bearing failure load of glass fibre/epoxy laminates. *Compos Part B Eng* 2009;40(3):197–205. <http://dx.doi.org/10.1016/j.compositesb.2008.11.005>.
- [9] Ascione F, Feo L, Maceri F. On the pin-bearing failure load of GFRP bolted laminates: an experimental analysis on the influence of bolt diameter. *Compos Part B Eng* 2010;41(6):482–90. <http://dx.doi.org/10.1016/j.compositesb.2010.04.001>.
- [10] Deng AZ, Zhao QL, Li F, Chen H. Research on bearing capacity of single tooth to

- composite pre-tightened teeth connection. *J Reinf Plastics Compos* November 2013;32(21):1603-13.
- [11] Catche S, Piquet R, Lachaud F, Castanie B, Benaben A. Analysis of hole wall defects of drilled carbon fiber reinforced polymer laminates. *J Compos Mater* 2015;49(10):1223-40. <http://dx.doi.org/10.1177/0021998314532668>.
- [12] Persson E, Eriksson I, Zackrisson L. Effects of hole machining defects on strength and fatigue life of composite laminates. *Compos Part A Appl Sci Manuf* 1997;28(2):141-51.
- [13] Saleem M, Toubal L, Zitoune R, Bougherara H. Investigating the effect of machining processes on the mechanical behavior of composite plates with circular holes. *Compos Part A Appl Sci Manuf* 2013;55:169-77. <http://dx.doi.org/10.1016/j.compositesa.2013.09.002>.
- [14] R. F. Handschuh, G. D. Roberts, R. R. Sinnamon, D. B. Stringer, B. D. Dykas, L. W. Kohlman, Hybrid gear preliminary results application of composites to dynamic mechanical components, NASA TM 217630.
- [15] Black S. New aerocomposites niche: helicopter transmission gears?. *CompositesWorld*. Jan. 2015. <http://www.compositesworld.com/articles/new-aerocomposites-niche-helicopter-transmission-gears>.
- [16] Crews Jr JH. Bolt-bearing fatigue of a graphite/epoxy laminate, Joining of composite materials. *ASTM STP* 1981;749:131-44.
- [17] Smith PA, Pascoe KJ. Fatigue of bolted joints in (0/90) CFRP laminates. *Compos Sci Technol* 1987;29:45-69.
- [18] P. Grant, N. Nguyen, Bearing fatigue and hole elongation in composite bolted joints, in: Proceedings of the 49th annual forum of the AHS, St. Louis, Missouri, 1993.
- [19] Liu D, Gau W, Zhang K, Ying B. Empirical damage evaluation of graphite/epoxy laminate bolt joint in fatigue. *Theor Appl Fract Mech* 1993;19(2):145-50.
- [20] Wei J, Jiao G, Jia P, Huang T. The effect of interference fit size on the fatigue life of bolted joints in composite laminates. *Compos Part B Eng* 2013;53:62-8. <http://dx.doi.org/10.1016/j.compositesb.2013.04.048>.
- [21] Counts WA, Johnson WS. Bolt bearing fatigue of polymer matrix composites at elevated temperature. *Int J Fatigue* 2002;24(2):197-204.
- [22] Seike S, Takao Y, Wang W-X, Matsubara T. Bearing damage evolution of a pinned joint in CFRP laminates under repeated tensile loading. *Int J Fatigue* 2010;32(1):72-81. <http://dx.doi.org/10.1016/j.ijfatigue.2009.02.010>.
- [23] Riccio A, Mozzillo G, Scaramuzzino F. Stacking sequence effects on fatigue intra-laminar damage progression in composite joints. *Appl Compos Mater* 2013;20(3):249-73. <http://dx.doi.org/10.1007/s10443-012-9268-5>.
- [24] Sola C, Castanié B, Michel L, Lachaud F, Delabie A, Mermoz E. On the role of kinking in the bearing failure of composite laminates. *Compos Struct* 2016;141:184-93. <http://dx.doi.org/10.1016/j.compstruct.2016.01.058>.
- [25] Hwang W, Han KS. Fatigue of composites fatigue modulus concept and life prediction. *J Compos Mater* 1986;20(2):154-65.
- [26] Wu F, Yao W. A fatigue damage model of composite materials. *Int J Fatigue* 2010;32(1):134-8. <http://dx.doi.org/10.1016/j.ijfatigue.2009.02.027>.
- [27] Chandra R, Singh S, Gupta K. Damping studies in fiber-reinforced composites a review. *Compos Struct* 1999;46(1):41-51.
- [28] Erber T, Guralnick S, Michels S. Hysteresis and fatigue. *Ann Phys* 1993;224(2):157-92.
- [29] Bathias C. There is no infinite fatigue life in metallic materials, *Fatigue and Fracture of Engineering*. *Mater Struct* 1999;22(7):559-66.
- [30] Nijssen RPL. Fatigue life prediction and strength degradation of wind turbine rotor blade composites. Ph.D. thesis. Delft (: TU Delft, Delft University of Technology; 2006.
- [31] Barnard P, Butler R, Curtis P. The Strength-Life Equal Rank Assumption and its application to the fatigue life prediction of composite materials. *Int J Fatigue* 1988;10(3):171-7.
- [32] Thompson RJH, Ansell MP, Bonfield PW, Dinwoodie JM. Fatigue in wood-based panels. Part 2: property changes during fatigue cycling of OSB, chipboard and MDF. *Wood Sci Technol* 2005;39(4):311-25. <http://dx.doi.org/10.1007/s00226-004-0277-x>.